

Supplementary Information

Effect of PEG Pairing on the Efficiency of Cancer-Targeting

Liposomes

Phei Er Saw,^{†,‡} Jinho Park,[†] Eunbeol Lee,[†] Sukyung Ahn,[†] Jinju Lee,[§] Hyungjun Kim,[†] Jinjoo Kim,[†] Minsuk Choi,[†] Omid C. Farokhzad[‡] and Sangyong Jon^{†,*}

[†]KAIST Institute for the BioCentury, Department of Biological Sciences, Korea Advanced Institute of Science and Technology (KAIST), 291 Daehak-ro, Daejeon 305-701, Republic of Korea. [‡]Laboratory of Nanomedicine and Biomaterials, Department of Anesthesiology, Brigham and Women's Hospital Harvard Medical School, Boston, MA 02115, U.S.A. [§]School of Life Sciences, Gwangju Institute of Science and Technology, 123-Cheomdangwagi-ro, Gwangju 500-712, Republic of Korea.

Synthesis of APT_{EDB}-PEG₂₀₀₀-DSPE and APT_{EDB}-PEG₁₀₀₀-DSPE.

APT_{EDB} containing an additional cysteine residue was dissolved in dimethyl sulfoxide (DMSO), and Mal-PEG₂₀₀₀-DSPE and Mal-PEG₁₀₀₀-DSPE were dissolved in chloroform. The conjugation reaction was carried out at an APT_{EDB}:Mal-PEG₂₀₀₀-DSPE or APT_{EDB}:Mal-PEG₁₀₀₀-DSPE molar ratio of 1:2 under inert conditions for 12 h at room temperature (Fig. S1a). Molecular weights of all PEGs used in these experiments are shown in Figure S1b. Conjugates were purified by reversed-phase HPLC (Fig. S2), and conjugation efficiency was determined by MALDI-TOF analysis. For HPLC, all samples were dissolved in ACN:water at 1:1 ratio, pre-filtered using a 0.2 μ m PDVF syringe membrane. Water alone (A) and ACN:water at 9:1 (B) containing ammonium acetate (10 mM) were used for elution. The gradient was set as 50% to 100% for 40 min at flowing rate of 0.7 mL/min. For MALDI-TOF analysis, all samples were re-dissolved in methanol, and mixed with DHB matrix at a ratio of sample:matrix to 1:5 ratio.

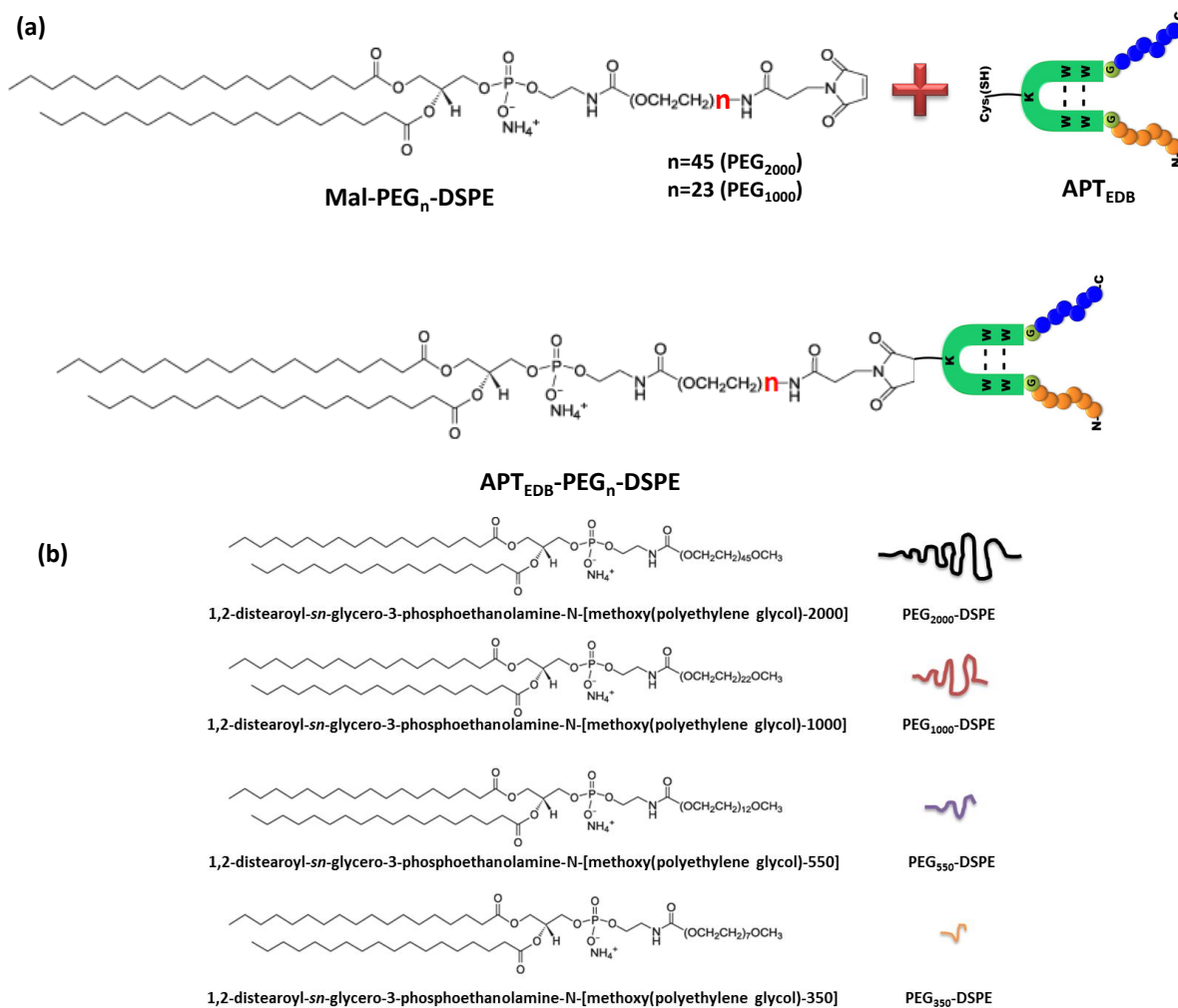


Fig. S1. (a) Schematic representation of the reaction between a cysteinylated APT_{EDB} and a maleimide-PEG phospholipids with molecular weights of 1000 and 2000 Da. (b) Chemical structures of the methoxy-capped PEGs with four different molecular weights (~350, 550, 1000, and 2000 Da).

Standard curve and loading efficiency of Dox in liposomes.

Doxorubicin hydrochloride was purchased from Boryung Pharmaceuticals (Seoul, South Korea). Dox was then dissolved in HBG buffer at 100 µg/mL concentration. The standard curve was measured with serial dilution, starting from 12.5, 6.25, 3.13, 1.56, 0.78 to 0.39 µg/mL. Fluorescence intensity of the standard Dox solution was measured at excitation wavelength of 480 nm and emission wavelength of 560-590 nm and plotted, leading to a linear standard curve with an R value of 0.9924 (Fig. S8). Next, the loading efficiency of Dox in liposomes was also measured using a following method. After Dox was loaded into each liposome, CL-4B (St. Louis, MO, USA) column was used to purify Dox encapsulating

liposomes from free Dox as mentioned previously in the Method section. The amount of Dox loaded in each liposome was calculated by measuring the fluorescence intensity of the collected liposomes. Approximately 7 wt% of Dox in average was loaded in each liposome (Table S1).

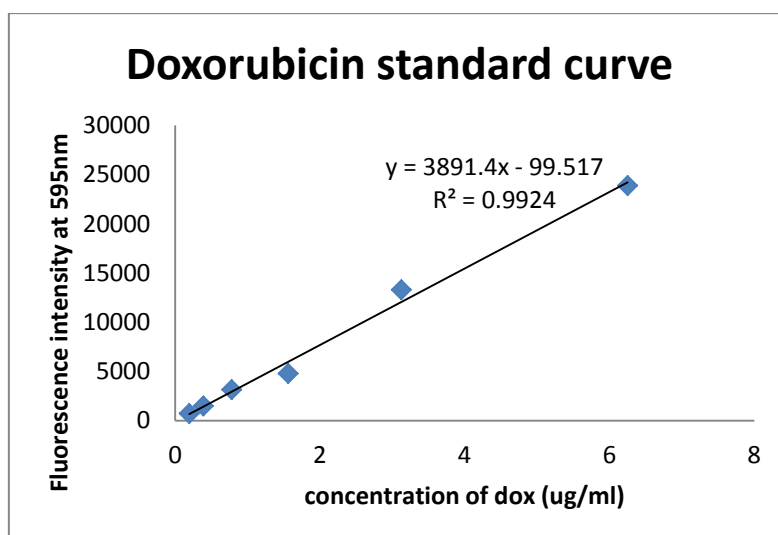


Fig. S2. A standard curve of Dox in PBS obtained by serial dilution: 12.5, 6.25, 3.13, 1.56, 0.78 and 0.39 $\mu\text{g/mL}$.

Table S1. The amount and encapsulation efficiency of Dox in five different liposomes (calculated for 5 mg of each liposome).

	LS	APT _{E_{DB}⁻ PEG_{2000/2000} LS}	APT _{E_{DB}⁻ PEG_{2000/1000} LS}	APT _{E_{DB}⁻ PEG_{1000/1000} LS}	APT _{E_{DB}⁻ PEG_{1000/550} LS}
Average reading	5366.785	5409.01	5476.425	5574.83	5598.305
Amount of encapsulation	1.404713	1.415564	1.432888	1.458176	1.464209
% encapsulation efficacy	7.023567	7.077822	7.164442	7.290881	7.321044

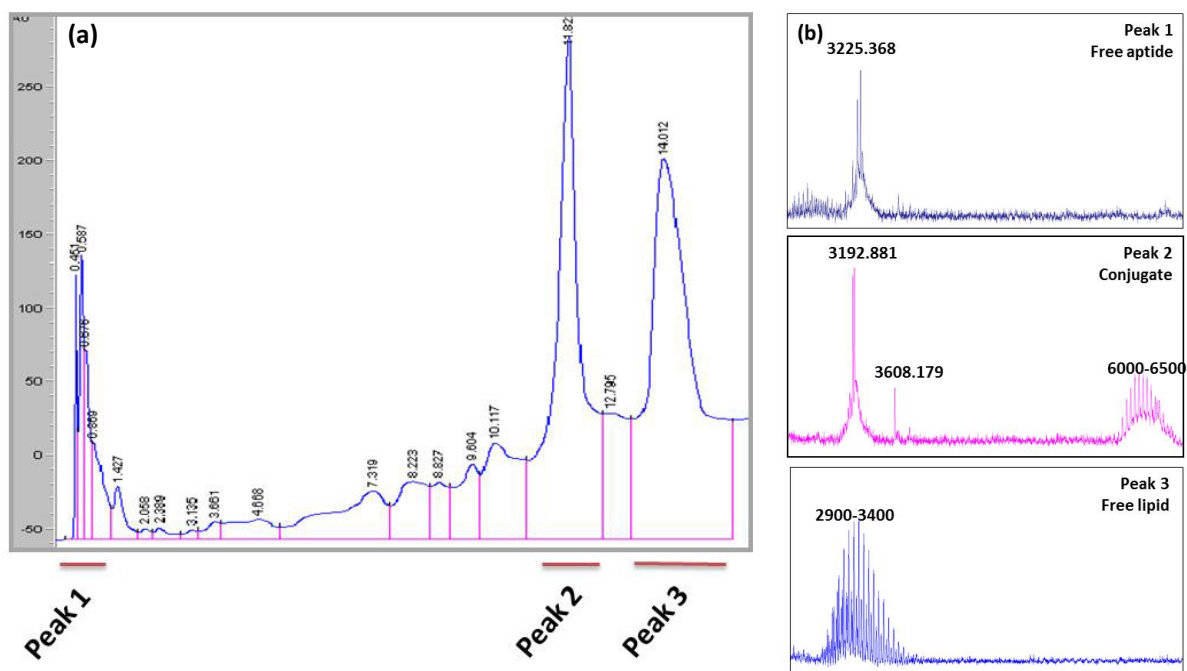
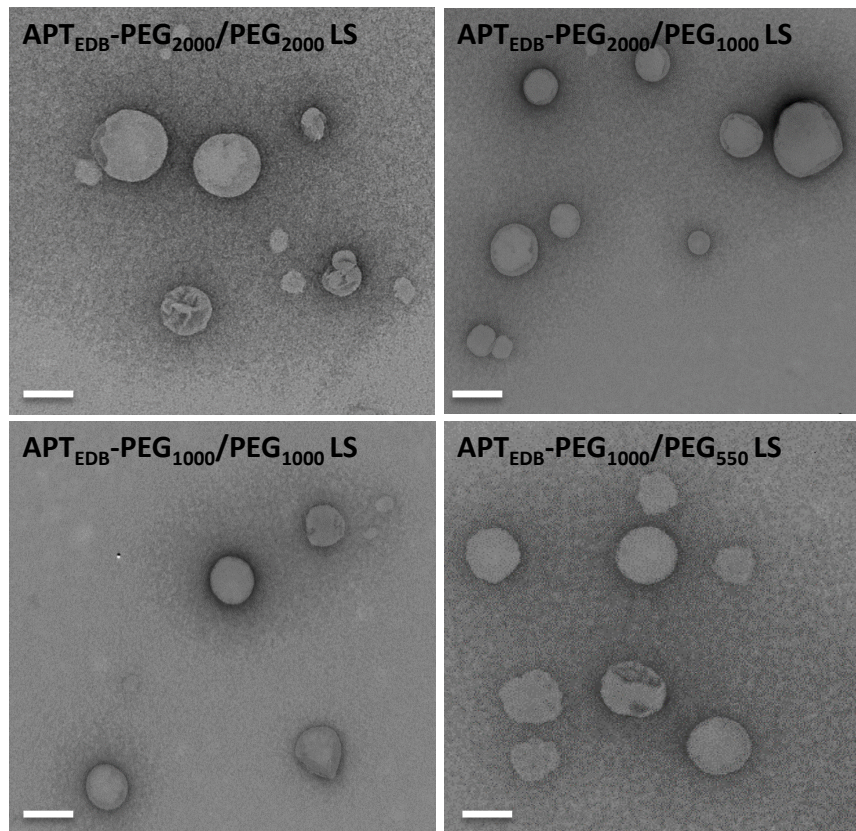


Fig. S3. (a) A HPLC profile of the APT_{EDB}-PEG₂₀₀₀-DSPE conjugate. (b) MALDI-TOF analysis of the three major peak fractions (Peaks 1, 2, and 3) shown in (a). Peak 1 corresponds to free APT_{EDB} ($M_w \sim 3300$); Peak 2 ($M_w \sim 6000-6500$) corresponds to APT_{EDB}-PEG₂₀₀₀-DSPE conjugate; Peak 3 ($M_w \sim 2900-3400$) corresponds to PEG₂₀₀₀-DSPE.

Characterization of liposomes by dynamic light scattering (DLS) and transmission electron microscopy (TEM).

All the liposomes (APT_{EDB}-PEG₂₀₀₀/PEG₂₀₀₀ LS, APT_{EDB}-PEG₂₀₀₀/PEG₁₀₀₀ LS, APT_{EDB}-PEG₁₀₀₀/PEG₁₀₀₀ LS and APT_{EDB}-PEG₁₀₀₀/PEG₅₅₀ LS) were analyzed with respect to morphology and size by TEM and DLS, respectively (Fig. S3). For DLS, each sample was first diluted to a concentration of 1 mg/mL before being subjected for analysis. All readings were taken in three runs, with 50 readings taken in each run. For TEM analysis, 5 μ L of each liposomal system was left to dry overnight on a carbon-mesh coated TEM grid. The samples were then stained with 2% uranyl acetate for 5 min, washed out with distilled water twice, and left to dry before analysis.



	Size (nm) \pm S.D.
APT_{EDB}-PEG₂₀₀₀-DSPE PEG₂₀₀₀	138.7 \pm 2.9
APT_{EDB}-PEG₂₀₀₀-DSPE PEG₁₀₀₀	112.1 \pm 0.8
APT_{EDB}-PEG₁₀₀₀-DSPE PEG₁₀₀₀	117.5 \pm 1.7
APT_{EDB}-PEG₁₀₀₀-DSPE PEG₅₅₀	126.7 \pm 1.3

Fig. S4. Characterization of four liposomes by TEM and DLS: APT_{EDB}-PEG₂₀₀₀/PEG₂₀₀₀ LS, APT_{EDB}-PEG₂₀₀₀/PEG₁₀₀₀ LS, APT_{EDB}-PEG₁₀₀₀/PEG₁₀₀₀ LS and APT_{EDB}-PEG₁₀₀₀/PEG₅₅₀ LS. Scale bars denote 100 nm.

Selection of EDB-positive cells.

Expression of the EDB domain of fibronectin in U87MG (human glioblastoma), SCC-7 (murine mouth carcinoma) and PC3 (human prostate cancer) cell lines was determined *in vitro* by conventional RT-PCR and qRT-PCR, and *in vitro* and *ex vivo* by immunocytochemistry.

(i) qRT-PCR

After collecting cells, total RNA was isolated using a RiboEx and GeneAll RNA isolation kit and reverse transcribed to yield cDNA. The EDB domain of fibronectin was detected in cDNA samples using the primer pair 5'-AAC TCA CTG ACC TAA GCT TT-3' (forward) and 5'-CGT TTG TTG TGT CAG TGT AG-3' (reverse). The following thermocycling protocol was used for conventional RT-PCR: 94°C for 4 minutes (initial denaturation), followed by 30 cycles of 94°C for 30 minutes (denaturation), 55°C for 30 minutes and extension at 72°C for 1 minute, with a final extension at 72°C for 4 minutes[1]. The PCR products were analyzed by agarose gel electrophoresis on 1% gels, with nucleic acid staining using RedSafe pre-mix. For qRT-PCR, 1 µg of cDNA and 1 pmol of primer were added to 4 µl of distilled water and 5 µl of SYBR Green real-time mixture (Takara) before running the mixture on a Qiagen qRT-PCR machine, according to the manufacturer's protocol (Fig. S5a).

(ii) Immunocytochemistry and immunohistochemistry

Cells or tumor tissue were first washed with PBS and then fixed with 4% PFA for 30 minutes at room temperature. After washing twice with PBS, the samples were incubated with PBST (PBS containing 0.1% Tween-80) for 5 minutes. After rinsing once with PBS, samples were blocked by incubating with 2% bovine serum albumen (BSA) for 1 hour at room temperature. Samples were then incubated overnight at 4°C with anti-BC-1 primary antibody (diluted 1:1000 in 1% BSA; Santa Cruz Biotechnology, Santa Cruz, CA, USA), which detects the fibronectin EDB domain. After washing with PBS, samples were incubated for 1 hour at room temperature with fluorescein isothiocyanate (FITC)-conjugated anti-mouse IgG secondary antibody, diluted 1:1000 in 1% BSA. After washing three times with PBS, samples were mounted on glass slides with Dako mounting medium for viewing under a confocal microscope (Fig. S5b).

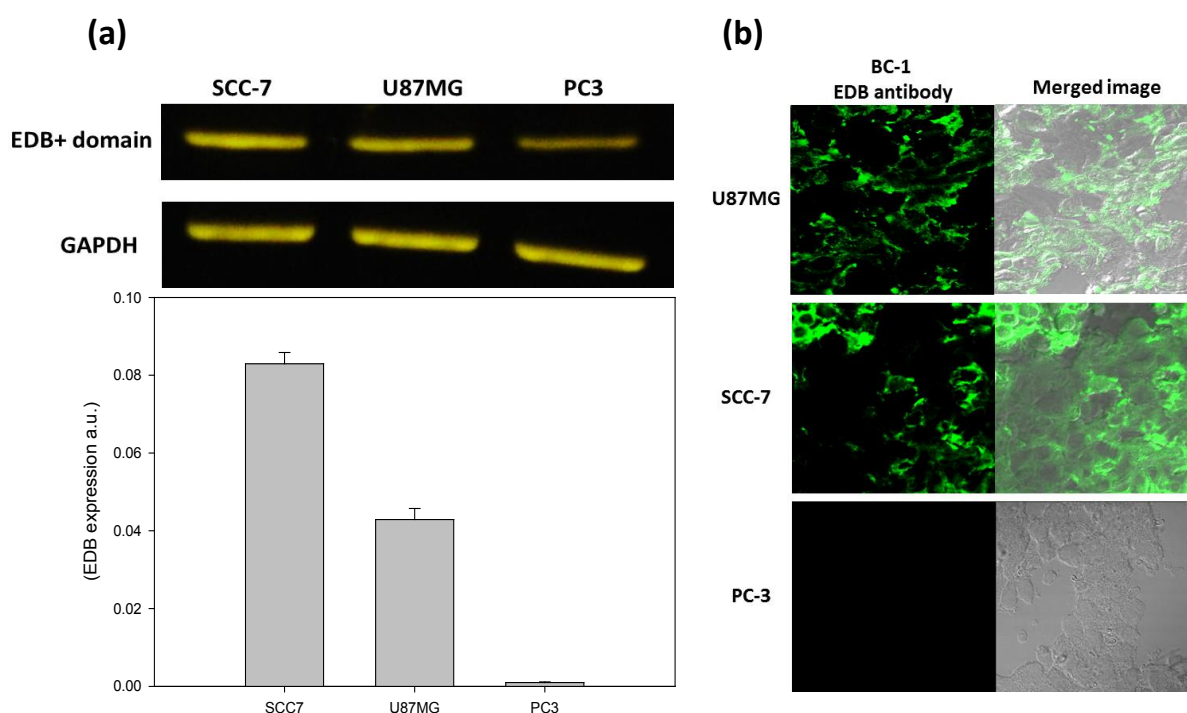


Fig. S5. (a) Detection and quantification of EDB expression in SCC-7, U87MG, and PC-3 cells by RT-PCR (top) and qRT-PCR (bottom). SCC-7 showed the highest EDB expression followed by U87MG while PC-3 cells showed marginally minimal expression of EDB. (b) *Ex vivo* assessment of EDB expression levels by immunohistochemistry in U87MG and PC-3 xenograft models and the SCC-7 allograft model. Rabbit anti-mouse EDB specific BC-1 primary antibody was used and FITC conjugated anti-rabbit IgG secondary antibody was used.

***In vitro* uptake of $APT_{EDB-PEG_{2000}/PEG_{2000}}$ LS, $APT_{EDB-PEG_{2000}/PEG_{1000}}$ LS, $APT_{EDB-PEG_{1000}/PEG_{1000}}$ LS, and $APT_{EDB-PEG_{1000}/PEG_{550}}$ LS in EDB-positive and EDB-negative cells.**

For cellular uptake experiments, $APT_{EDB-PEG_{2000}/PEG_{2000}}$ LS, $APT_{EDB-PEG_{2000}/PEG_{1000}}$ LS, $APT_{EDB-PEG_{1000}/PEG_{1000}}$ LS, and $APT_{EDB-PEG_{1000}/PEG_{550}}$ LS were labeled with 0.5% rhodamine-DSPE. U87MG cells were grown to confluence on sterilized coverslips and then treated with liposomes at a concentration of 100 $\mu\text{g/ml}$ for 1 hour at 37°C. Cells were then washed with PBS, fixed with 4% PFA, and mounted on glass slides for confocal microscopy (Fig. S6). To ensure that uptake was solely attributable to EDB-specific binding, we performed similar uptake experiments using scrambled aptide (ATP_{scr})–conjugated liposomes and non-targeting liposomes as negative controls (Fig. S7).

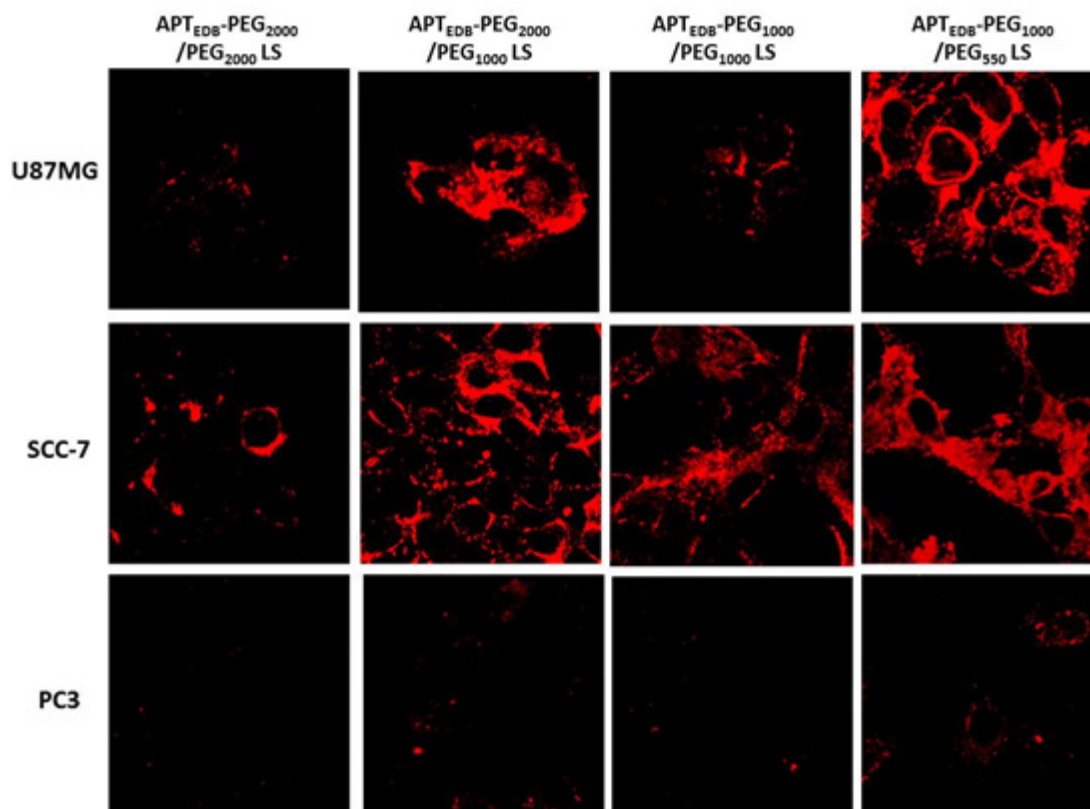


Fig. S6. *In vitro* uptake of APT_{E_{EDB}}-PEG₂₀₀₀/PEG₂₀₀₀ LS, APT_{E_{EDB}}-PEG₂₀₀₀/PEG₁₀₀₀ LS, APT_{E_{EDB}}-PEG₁₀₀₀/PEG₁₀₀₀ LS and APT_{E_{EDB}}-PEG₁₀₀₀/PEG₅₅₀ LS in EDB-positive (U87MG and SCC-7) and EDB-negative (PC3) cell lines. The highest uptake was seen in APT_{E_{EDB}}-PEG₂₀₀₀/PEG₁₀₀₀ LS and APT_{E_{EDB}}-PEG₁₀₀₀/PEG₅₅₀ LS in U87MG and SCC-7 cell lines, whereas minimal uptake was seen in the PC3 cell line, indicating the specificity of EDB targeting.

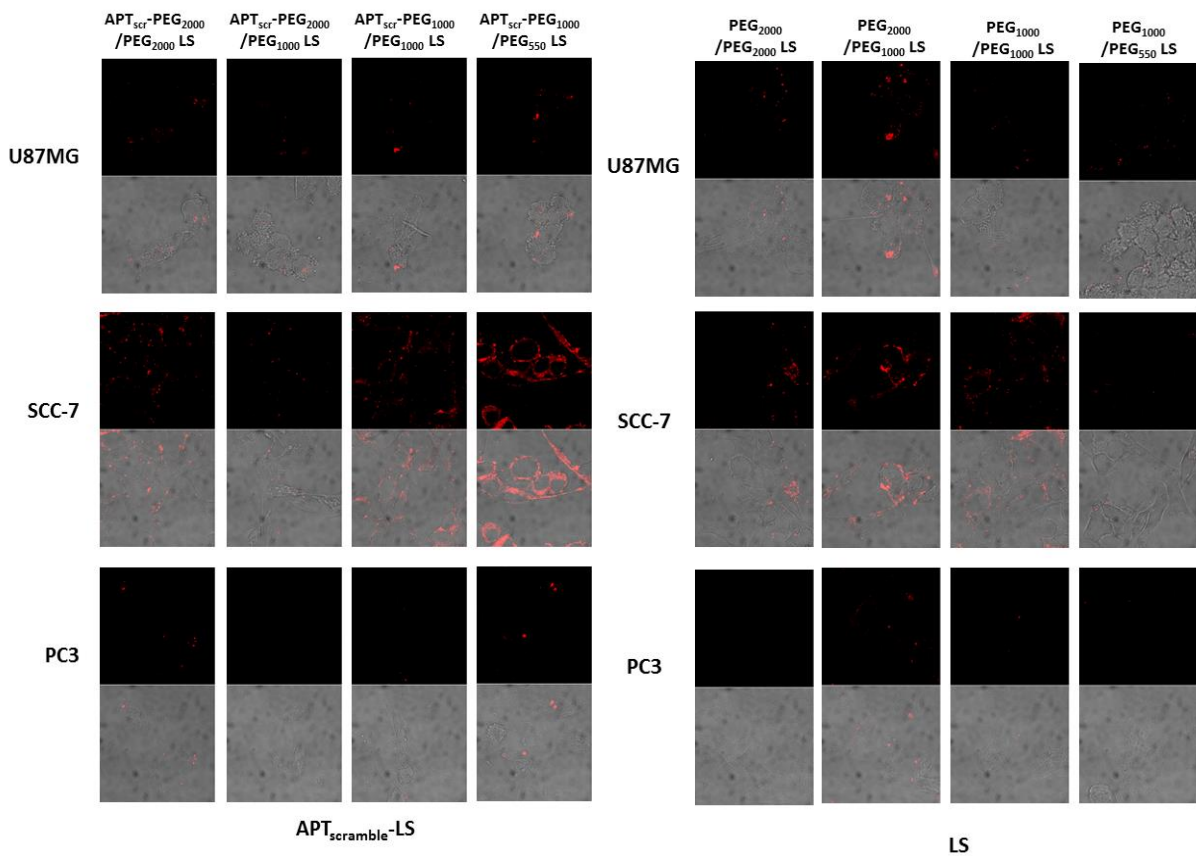


Fig. S7. Confirmation of specific targeting by APT_{EDB}-liposomes, showing minimal uptake of scrambled aptide (APT_{scr})-conjugated liposomes and non-targeting liposome in all cell lines tested (SCC-7, U87MG and PC-3).

***In vitro* co-staining with ER-, Mito-, and Lyso-Tracker.**

U87MG and SCC-7 cells were grown to confluence on glass slide-containing 24-well plates. Cells in serum-free media were treated for 1 hour with each liposome formulation, labeled with 0.1% rhodamine. Cells were treated with ER-, Mito-, and Lyso-Tracker according to the protocol provided by the manufacturer (Invitrogen Inc.). Cells were then washed with PBS, fixed with 4% PFA for 10 minutes, washed twice with PBS, and mounted on glass slides for confocal microscopy (Fig. S8).

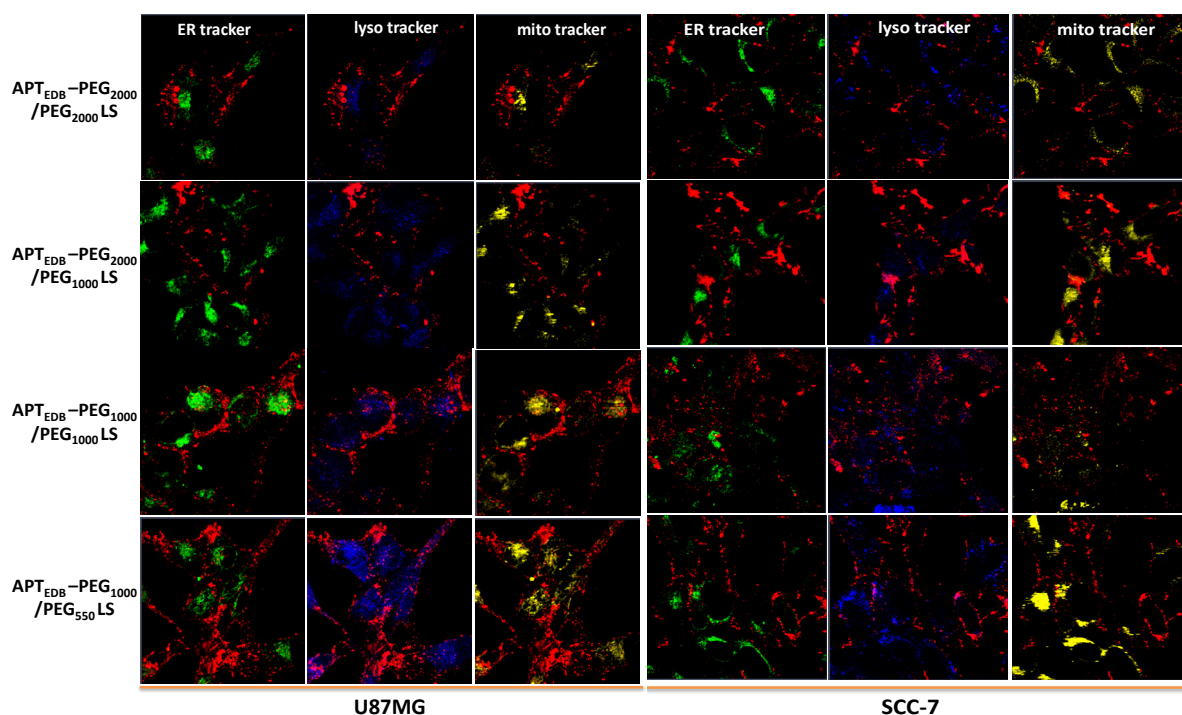


Fig. S8. Co-staining of all liposomes with ER-, Mito-, and Lyso-Tracker in U87MG and SCC-7 cell lines *in vitro*. All liposomes were uptaken in a similar manner indicating the same mechanism pathway for all APT_{EDB}-PEG₂₀₀₀/PEG₂₀₀₀ LS, APT_{EDB}-PEG₂₀₀₀/PEG₁₀₀₀ LS, APT_{EDB}-PEG₁₀₀₀/PEG₁₀₀₀ LS, and APT_{EDB}-PEG₁₀₀₀/PEG₅₅₀ LS.

Biodistribution of liposomes in the U87MG xenograft model

To determine the biodistribution of all the liposomal formulations *in vivo*, an U87MG xenograft model was made by injecting 5×10^6 of U87MG cells subcutaneously into Balb/c female nude mice. The liposomes were first labeled with either 0.5 wt% Alexa647-PEG₂₀₀₀-DSPE (for APT_{EDB}-PEG₂₀₀₀/PEG₂₀₀₀ LS and APT_{EDB}-PEG₂₀₀₀/PEG₁₀₀₀ LS) or Alexa647-PEG₁₀₀₀-DSPE (for APT_{EDB}-PEG₁₀₀₀/PEG₁₀₀₀ LS and APT_{EDB}-PEG₁₀₀₀/PEG₅₅₀ LS). The resulting dye-labeled liposomal formulations were then injected into mice *via* the tail vein. After 24 h, all vital organs (liver, heart, lung, spleen and kidney) and the tumor were excised and imaged with the Syngene Pxi® imaging system. All images were taken with a ten-second exposure time to ensure consistency in the data.

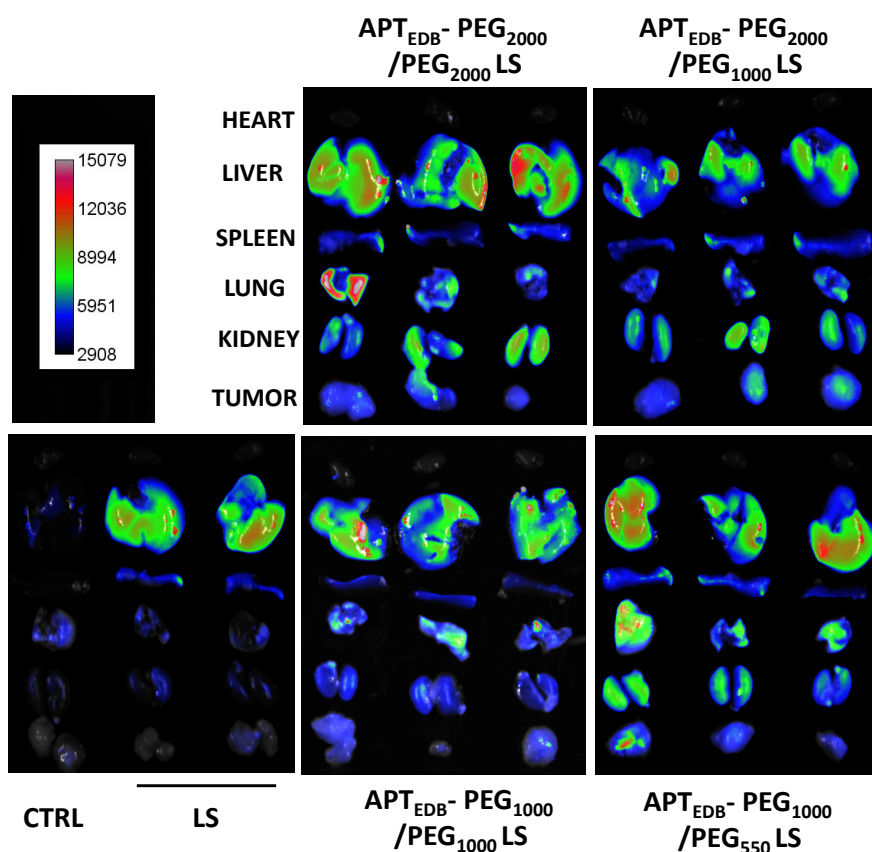


Fig. S9 Biodistribution of Alexa647-labeled liposome formulations in U87MG xenograft models. After tail vein injection of each liposome formulation, mice were euthanized at 24 h post injection and fluorescence images of vital organs and tumor tissues were taken using a Syngene Pxi® imaging system with 10 sec of exposure time (n = 3 for each group, s.e.). The highest fluorescence signal in the tumor area is seen for APT_{EDB}-PEG₂₀₀₀/PEG₁₀₀₀ LS group, followed by APT_{EDB}-PEG₁₀₀₀/PEG₅₅₀ LS.

Reference

1. Matsui S, Takahashi T, Oyanagi Y, Takahashi S, Boku S, Takahashi K, et al. Expression, localization and alternative splicing pattern of fibronectin messenger RNA in fibrotic human liver and hepatocellular carcinoma. *J Hepatol.* 1997; 27: 843-53.